BMC Medical Genomics

RESEARCH Open Access

# A novel frameshift variant leads to familial osteopetrosis with variable phenotypes in a Chinese Han consanguineous family

Mengxiao Liu[1,2,3†], Hao Zheng[4†], Zhixiang Li[1,2,3†], Runfei Pang[3], Yang Niu[1,2], Lei Yang[3], Zhenxiang Zhang[5*], Jianguo Xia[6*] and Xiuhong Pang[1,2,3*]

## Abstract

Osteopetrosis, a group of highly heterogeneous genetic bone disorders, is characterized by deafness, increased bone density, hepatosplenomegaly, pancytopenia and intellectual disability. Osteopetrosis can be divided into three subtypes: autosomal recessive osteopetrosis (ARO), intermediate autosomal recessive osteopetrosis (IARO), and autosomal dominant osteopetrosis (ADO). *CLCN7* has been reported to be the most common gene responsible for the ADO-II subtype. In this study, a novel variant, c.175dupA (p.Met59Asnfs*8), of *CLCN7* was identified in a Chinese Han consanguineous family with suspected ADO-II. The proband was homozygous for the p.Met59Asnfs*8 variant and exhibited multiple severe phenotypes, including deafness, short stature, brittle bones, optic atrophy, hepatosplenomegaly, intellectual disability, cleft palate and recurrent infection. However, except for the mother of the proband, who presented a series of clinical phenotypes caused by bone marrow failure, all the other family members who were heterozygous had no obvious abnormal phenotypes. Our study suggested that the novel variant p.Met59Asnfs*8 in *CLCN7* was very likely pathogenic factor in our suspected ADO-II family. The phenotypes of heterozygous carriers may be affected by incomplete penetrance. Loss of function of CLCN7 caused by nonsense-mediated mRNA decay (NMD) due to the frameshift variant was likely the underlying pathogenic mechanism. This study broadened the mutation spectrum of *CLCN7*, provided a foundation for timely and effective clinical intervention for related diseases, and demonstrates the importance of genetic counselling.

## Introduction

Osteopetrosis (OP), also called marble bone disease, is a group of genetic bone disorders characterized by increased bone density, hepatosplenomegaly, pancytopenia, hearing loss and intellectual disability [1]. To date, at least 13 genes have been associated with osteopetrosis, including *TCIRG1* (OMIM 604592), *CLCN7* (OMIM 602727), *TNFRSF11* (OMIM 602642), *TNFRSF11A* (OMIM 603499), *TNFRSF11B* (OMIM 602643), *OSTM1* (OMIM 607649), *SNX10* (OMIM 614780), *CTSK* (OMIM 601105), *LRP5* (OMIM 603506), *MITF* (OMIM 156845), *CAII* (OMIM 611492), *PLEKHM1* (OMIM 611466), and *SLC4A2* (OMIM 109280) [2, 3]. According to the

†Mengxiao Liu, Hao Zheng and Zhixiang Li contributed equally to this work.

Xiuhong Pang is the first corresponding author, Jianguo Xia is the second corresponding author; and Zhengxiang Zhang is the third corresponding author.

*Correspondence:
Zhenxiang Zhang
kafeimao1982@126.com
Jianguo Xia
shjxct@163.com
Xiuhong Pang
pxhzxy@163.com

Full list of author information is available at the end of the article

**Keywords** *CLCN7*, Autosomal dominant osteopetrosis (ADO), Consanguineous family, Frameshift variant, Loss of function

inheritance mode and severity of the phenotypes, OP can be classified into three major subtypes: autosomal recessive osteopetrosis (ARO), intermediate autosomal recessive osteopetrosis (IARO) and autosomal dominant osteopetrosis (ADO) [4]. ARO is the most malignant subtype of OP, with death occurring before 10 years of age in all patients and a high mortality rate in infancy [5, 6]. ADO is benign with mild clinical symptoms, and patients have a normal lifespan [4, 7]. The degree of malignancy of IARO is intermediate between that of ADO and ARO [4]. Mutations in *TCIRG1*, *TNFRSF11,CAII,CLCN7,OSTM1,PLEKHM1,TNFRSF11A,SNX10,SLC4A2*, and *CTSK* are associated with ARO, mutations in *TCIRG1* account for approximately 50% of cases [3]. In addition, ADO is caused mostly by mutations in *CLCN7,LRP5* and *PLEKHM1* [4, 7].

ADO can be divided into type I (ADO-I, OMIM 607634) and type II (ADO-II, OMIM 166600) according to the pathogenic gene, clinical symptoms and auxiliary examination results [1]. ADO-I is characterized by mild extensive osteopetrosis, especially in the skull and cranial vault; a relatively normal spine; and a dense pedicle of the vertebral arch [5]. Most ADO-I cases are thought to be caused by mutations in *LRP5* [8]. ADO-II (OMIM 166600), also known as Albers–Schonberg disease, is the most common type of osteopetrosis, with an incidence of approximately 1:20000, and usually occurs in adolescence or adulthood [9]. ADO-II is highly heterogeneous, ranging from asymptomatic to a severe phenotype [1, 10]. The main pathological changes are usually limited to skeletal system; common changes include bone pain, arthritis, osteomyelitis of the mandible, tooth eruption disorder, missing teeth and malocclusion, pathological fracture, delayed union, bone nonunion and postoperative secondary infection [1]. Cranial nerve compression and bone marrow failure are rare, and life expectancy is normal [1, 11]. Radiographically, the vertebral endplate is thickened, and the vertebral body exhibits a "sandwich" shape, also known as the "Rugger–Jersey spine". The metaphyseal widening of the extremities shows "bottle sign" changes, and the iliac bone is a "bone-in-bone" phenomenon [1, 10, 12]. Mutations in the *CLCN7* gene (chloride voltage-gated channel 7, OMIM 602727) are responsible for approximately 75% of ADO-II cases [11, 13]. The penetrance of ADO II is estimated to be between 60% and 80%, and the penetrance of *CLCN7*-dependent ADO-II is only approximately 44% [14]. Therefore, patients carrying the same heterozygous mutation in *CLCN7* can present with normal or abnormal clinical phenotypes [1, 9].

*CLCN7*, the most common gene associated with ADO-II, encodes the $2Cl^-/1H^+$ reverse membrane transporter CLCN7, which has 805 amino acids and includes three motifs and two cytoplasmic cystathionine-β-synthase (CBS) domains [11]. CLCN7 is widely expressed in many tissues and organs in the body, such as the spleen, kidney, and bone marrow, especially in lysosomal and osteoclast ruffled membranes [7]. The CBS domains, encoded by bases 631–799, are responsible for maintaining the slow voltage power of chloride ion channels and activating the gating protein to create an outwards current [14]. Three important motifs, followed by the CBS domains, begin at base 203 and end at base 516, a region with a selective filtering function [7, 11]. Each subunit contains its own independent ion permeation pathway and has relatively independent functions [15, 16]. When V-ATPase pumps protons into lysosomes, osteoclasts and other cavities, CLCN7 provides the required $Cl^-$ through its function as a slow voltage-gated $2Cl^-/1H^+$ channel transport protein, maintaining electrical neutrality between the inside and outside of cells [14, 15, 17, 18]. Mutations and aberrant expression of *CLCN7* lead to lysosomal storage disease and OP [19]. To date, more than 300 *CLCN7* mutations have been identified worldwide in the database ClinVar, which are responsible for approximately 80% of ADO-II cases and 17% of ARO cases [3, 20].

In this study, we identified a novel *CLCN7* truncation variant in a specific consanguineous family with suspected ADO-II. Our results suggested that the novel variant in *CLCN7* was very likely the pathogenic factor in this family and that the phenotype caused by this variant might have incomplete penetrance.

## Materials and methods

### Editorial policies and ethical considerations

All the subjects or their legal guardians provided written, informed consent to participate in this study. Identifying information will not be included in the manuscript unless the information is essential for scientific purposes. Documented permission for the use of identifiable patient images was obtained by a patient consent form signed by the patients or their legal guardians. This study was approved by the Ethics Committee of the Affiliated Taizhou People's Hospital of Nanjing Medical University (KY202012301; 22 October, 2020) and complied with the Declaration of Helsinki.

### Subjects and clinical examinations

All affected (proband IV-1 and mother III-3) and unaffected (consanguineous father III-2, paternal aunt III-1,

and younger brother IV-2) members of family P-S15 were recruited by the Department of Otolaryngology-Head and Neck Surgery, the Affiliated Taizhou People's Hospital of Nanjing Medical University (Fig. 1a). A comprehensive clinical history was obtained, and a detailed physical examination was performed, with a focus on audiological, skeletal, nasal, pharyngeal, hepatic, splenic, haematic, ophthalmologic, mental development and infection history.

Hearing loss was confirmed by otoscopy, pure-tone audiometry (PTA), immittance, and auditory brainstem response (ABR). Height and weight were measured via standard methods and classified according to the Chinese Han population standard issued by the General Administration of Sport of China in 2022 (https://www.sport.gov.cn/n315/n329/c24335066/content.html). Blood was colle cted from all family members for routine and biochemical tests to rule out blood system diseases. If necessary,

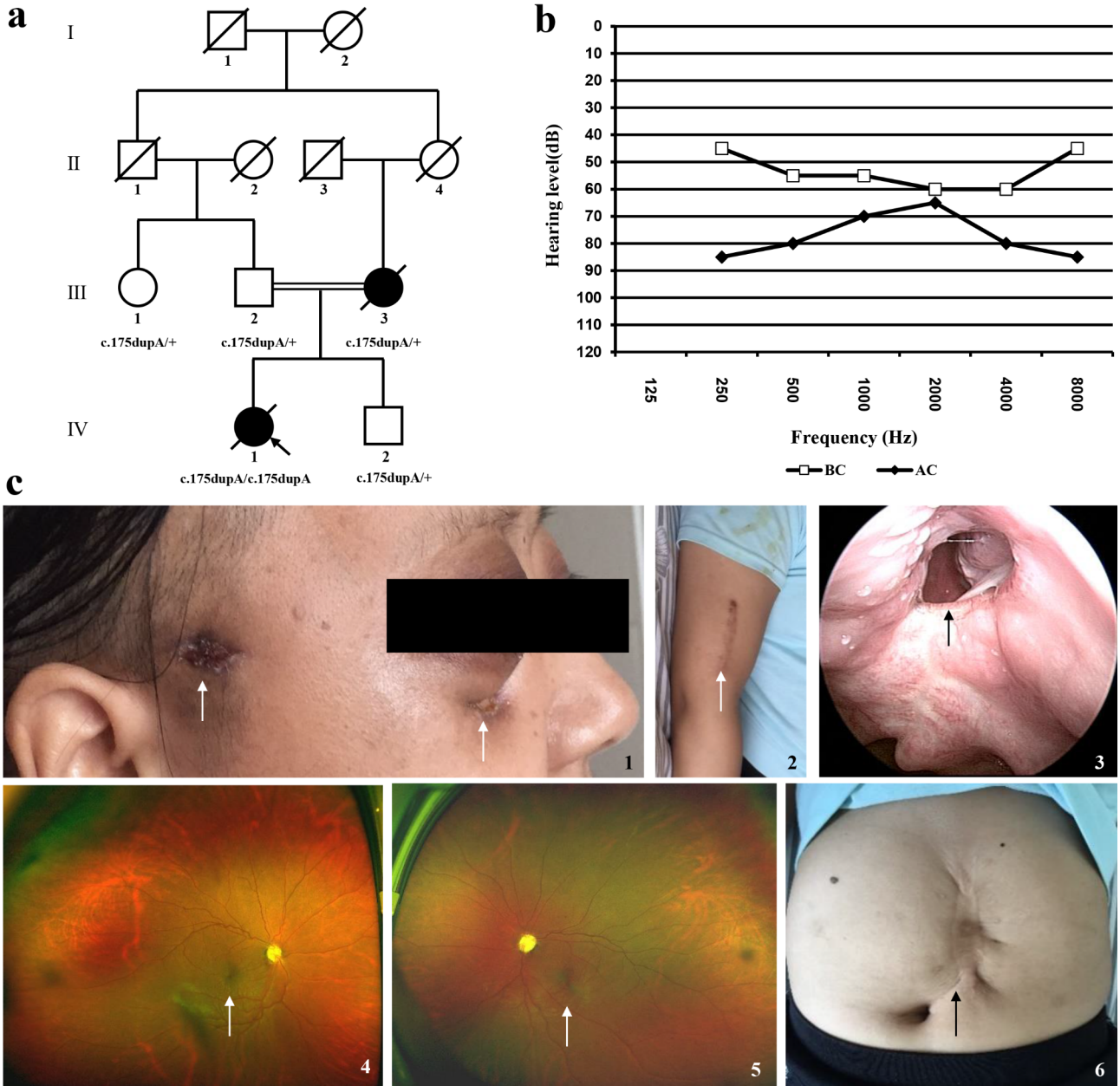


**Fig. 1** Pedigree, audiograms and characteristic phenotype of the proband. (**a**) Pedigree. Proband (IV-1) was pointed by the black arrow. (**b**) Audiograms. Small square curve: bone conduction (BC); Small black diamond curve: air conduction (AC). (**c**) Characteristic phenotype. (c1) temporal-facial fistula and abscess (white arrows). (c2) postoperative scar with pigmentation of right upper arm fracture (white arrows). (c3) cleft palate by electronic laryngoscopy (black arrow). (c4-5) retinal macular degeneration performed by fundus mirror (white arrows). (c6) old central abdominal scar after splenectomy (black arrow)

further bone marrow puncture and pathological examination could be performed. Abdominal abnormalities were screened by colour Doppler ultrasound. Cranial and thoracic conditions were evaluated via computed tomography and digital radiography. The malformation of inner ear development was excluded by high-resolution CT (HRCT) and nuclear magnetic resonance imaging (MRI). Fundus lesions were detected via fundus microscopy. Otorhinolaryngologic malformations were identified via electronic endoscopy.

#### Mutation screening of all related known genes by targeted NGS

Genomic DNA was extracted from whole blood using a DNA Extraction Kit (QIAGEN, CA, USA). All 406 known deafness genes (Panel V4, Hereditary hearing loss) and 812 osteology genes (Panel V2, Osteology System, including 13 osteosclerosis-related genes) were screened via targeted next-generation sequencing (targeted NGS) using the MyGenostics gene enrichment system (MyGenostics, Boston, MA, USA) and the Illumina Nova6000 sequencer (Illumina, San Diego, CA, USA) to obtain paired reads of 150 bp according to the manufacturer's protocol. The average sequencing depth was required to be greater than 300×, and the target area coverage was required to be greater than 98% for Q10 and 95% for Q30. The high-quality reads were aligned to hg19 using BWA software, and variants were called using the Genome Analysis Toolkit (GATK), both with the default parameters.

The pLI score of suspected pathogenic gene was obtained via the database gnomAD. The identified SNPs and InDels were annotated with the Exome-assistant program. MagicViewer was used to view the short-read alignment and validate the candidate SNPs and InDels. Nonsynonymous variants with a maximum minor allele frequency (MAF) less than 0.001 in the public databases $Geno_2MP$ (original Exome Variant Server), 1000 Genomes, and gnomAD were evaluated via software tools such as PROVEAN (cut-off score <-2.5), SIFT (cut-off score < 0.01), MutationTaster and PolyPhen-2, and pathogenicity was predicted according to the ACMG guideline criteria. A search of the $Geno_2MP$, gnomAD, ClinVar, 1000 Genomes and Franklin databases was performed to determine whether the variants were novel.

#### Validation by sanger sequencing

Suspected pathogenic variant of *CLCN7* was verified by Sanger sequencing in the proband (IV-1) and her consanguineous parents (III-2 and III-3), paternal aunt (III-1) and brother (IV-2) (forward primer: 5'-GTTTGTGT CTCAAGACCCAG-3'; reverse primer: 5'-TCAGGGAA GATTTCCTTGG-3'). The variant was also screened in 400 Chinese Han controls with normal hearing and no skeletal diseases to evaluate the allelic frequency (< 0.001) in the same ethnic population.

## Results

### Clinical characteristics

Family P-S15 was a consanguineous family in which the paternal grandfather and maternal grandmother of the proband were siblings (Fig. 1a). The proband (IV-1), a 30-year-old female, presented with short stature (150 cm and 46 kg; average height and weight for Chinese women aged 30–34 y: 159.1 cm and 58 kg), intellectual disability, mixed hearing loss (Fig. 1b), exophthalmos and recurrent temporal–facial infection (Fig. 1c), fracture of the right upper arm (Fig. 1c), cleft palate (Fig. 1c), and visual impairment and macular degeneration detected during funduscopic examination (Fig. 1c). The proband developed severe anaemia and thrombocytopenia when she was approximately 2 years old. Due to these conditions in combination with splenomegaly, splenectomy was performed on the proband at the age of 3 years (Fig. 1c; Table 1); encouragingly, her haematological symptoms improved significantly after the surgical intervention (Table 1). Imaging findings revealed fracture of the right upper arm and proximal phalanx of the left middle finger (Fig. 2a and b); increased bone density (Fig. 2); scoliosis and "sandwich" appearance of the vertebrae (Fig. 2c); an Erlenmeyer flask deformity of the tibia and fibula (Fig. 2d); skull thickening (Fig. 2e and f); ossification of the ethmoid, sphenoid and maxillary sinuses (Fig. 2g and h); hammer–anvil joint fixation and tympanosclerosis (Fig. 2i and j); and agomphiasis and irregular tooth alignment (Fig. 2k and l). A secondary temporofacial fistula and recurrent abscess developed after right infraorbital cyst excision (Fig. 1c), which was consistent with the diagnosis of chronic maxillary osteomyelitis. Recurrent temporofacial infection invaded the brain via haematogenous factors, and the proband ultimately died at the age of 33 due to uncontrolled intracranial infection. However, the patient's family did not consent to a bone marrow biopsy.

Severe anaemia, leukopenia and thrombocytopenia were diagnosed via haematological tests in the proband's mother (III-3) at approximately 40 years of age (Table 1). Bone marrow failure was identified as the underlying cause of her clinical symptoms via bone marrow aspiration (Fig. 3a). Unfortunately, she died at 55 years of age from an intracranial haemorrhage caused by thrombocytopenia (Fig. 3b and c). No bone-related abnormal phenotypes, such as increased bone density or ossification of the paranasal sinuses, as observed in the proband, were detected in the mother.

**Table 1** Clinical findings in the proband IV-1 and her mother III-3

| **General information** | **IV-1** | | **III-3** |
|---|---|---|---|
| Gender | female | | female |
| Onset age | 3y | | 40y |
| Age at admission | 3y | | - |
| Death (age) | 30y | | 55y |
| **Clinical features** | **IV-1** | | **III-3** |
| Developmental delay | short stature; mental retardation | | No |
| Hearing loss | Yes | | No |
| Facial abnormality | exophthalmos; temporal-facial fistula and abscess | | No |
| Visual impairment | Yes | | No |
| Palate cleft | Yes | | No |
| Dental problem | agomphiasis; irregular teeth alignment | | No |
| Osteomyelitis | Yes | | No |
| Skeletal symptom | bone fracture | | inger skeletal deformity |
| Splenomegaly | Yes | | Yes |
| **Imaging findings** | **IV-1** | | **III-3** |
| Chest X-ray | increased bone density; scoliosis; "sandwich" appearance of vertebrae | | NA |
| Long-Bone X-ray | increased bone density; fracture of right upper arm; Erlenmeyer flask deformity of tibia and fibula | | NA |
| Hand X-ray | fracture of proximal phalanx of left middle finger | | NA |
| Cranial CT | skull thickening, palate cleft, agomphiasis, irregular teeth alignment; poor sinus gasification; the hammer-anvil joint fixation; tympanosclerosis; bone sclerosis of the maxilla and mastoid | | intracranial hemorrhage |
| **Laboratory test** | **IV-1** | | **III-3** |
| | **pre-operation** | **post-operation** | |
| RBC (3.8–5.1 × $10^{12}$/L) | 3.0 | 3.9 | 3.5 |
| WBC (3.5–9.5 × $10^{9}$/L) | 2.9 | 10.2 | 2.5 |
| PLT (125–350 × $10^{9}$/L) | 30 | 110 | 20 |
| Hb (115–150 g/L) | 59 | 101 | 71 |
| Bone marrow aspiration | NA | | bone marrow failure |

RBC, Red blood cell; WBC, White blood cell; PLT, Platelets; Hb, Hemoglobin; NA, Not available

### Mutation analysis

A novel variant, c.175dupA (p.Met59Asnfs*8) in *CLCN7* (NM_001287.6) was identified as a likely pathogenic variant associated with the phenotypes in this family. Homozygous p.Met59Asnfs*8 was identified in the proband, who presented with a series of OP phenotypes (Figs. 1a and 4a). The consanguineous parents (III-2 and III-3), paternal aunt (III-1), and younger brother (IV-2) all carried heterozygous variant. Except for the proband's mother (III-3), who had a range of clinical manifestations of myelodysplasia, no other carriers had abnormal clinical phenotypes (Figs. 1a and 4a).

Through the insertion of an adenine nucleotide into the 175th coding base of *CLCN7*, the variant p.Met59Asnfs*8 change the amino acid sequence beginning at codon 59, resulting in termination of protein expression at codon 66 (Fig. 4b). The variant was predicted to be "disease causing", "changed amino acid sequence", "affect protein features", "changed splice site", and "caused NMD" by the software tool MutationTaster. According to the ACMG guideline criteria, this variant was predicted to be "likely pathogenic" (PVS1 and PM2) by the software tool Franklin. The variant was not found in 400 ethnically matched normal controls by Sanger sequencing and has not been reported in the $Geno_2M$, gnomAD, ClinVar, 1000 Genomes or Franklin databases.

## Discussion

A novel frameshift variant, p.Met59Asnfs*8, in the OP-related gene *CLCN7* was identified in a highly suspected OP family and was very likely the genetic cause of OP. Through the insertion of an adenine nucleotide into the 175th coding base of *CLCN7*, the c.175dupA variant changed the subsequent amino acid sequence beginning at codon 59, which terminated translation at codon 66, resulting in the complete loss of the two CBS and three motif domains (Fig. 4) [11]. This frameshift variant most likely induced rapid degradation of mRNA containing premature stop codons by the mRNA surveillance mechanism NMD [21]. In addition, although the pLI of the *CLCN7* gene was zero, loss of function (LOF) is still considered a potential pathogenic mechanism for many pathogenic stop-gain (26.8%, 11/41) and frameshift (20.8%, 16/77) mutations in database gnomAD.

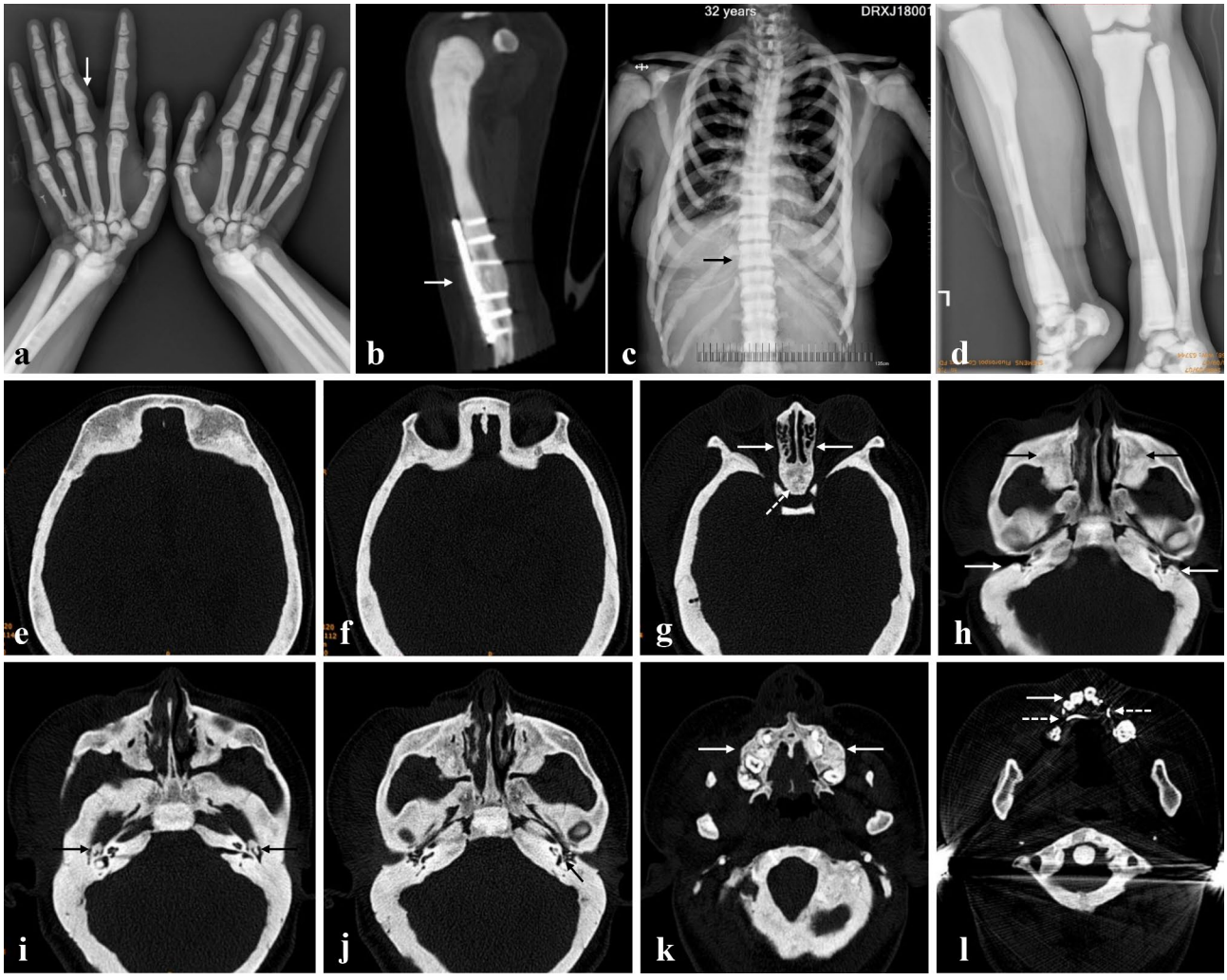


**Fig. 2** Imaging findings of the proband (IV-1). (**a**-**d**) X-ray manifestation. The generalized increase in the bone density of the rib, spine, humerus, tibia, fibula. (a) Malunion of fracture of proximal phalanx in left middle finger. (**b**) Fracture of right upper arm with internal fixation (white arrows). (**c**) Spinal scoliosis and "sandwich" appearance of vertebrae (black arrow). (**d**) Erlenmeyer flask deformity of tibia and fibula. (e-l) Computed Tomography manifestation. (**e**-**f**) Skull thickening. (**g**) Poor sinus gasification (arrows). (**h**) Bone sclerosis of the maxilla (black arrows) and mastoid (white arrows). (**i**-**j**) The hammer-anvil joint fixation and tympanosclerosis (black arrows). (**k**-**l**) Irregular tooth alignment and agomphosis (white arrows)

*Clcn7*$^{-/-}$ mice have previously been reported to develop severe osteopetrosis due to the inability of osteoclasts to secrete acid and thus to lyse bone [22]. Therefore, we speculated that the complete loss of CLCN7 function caused by the p.Met59Asnfs*8 variant, resulting in disordered chloride channel transport and the inability of lysosomes and osteoclasts to obtain chloride ions for acidification, which may be the underlying pathogenic mechanism of this variant (Fig. 4b) [15–17, 19]. However, additional pathogenic evidence will need to be confirmed by further functional studies.

In our study, the proband's mother (III-3), who was heterozygous for the p.Met59Asnfs*8 variant of *CLCN7*, developed pancytopenia, secondary splenomegaly and bone marrow failure at approximately 40 years of age (Fig. 3a; Table 1). It was likely not a coincidence that two family members carrying a frameshift variant in *CLCN7* experienced pancytopenia. Pancytopenia in the mother (III-3), who was heterozygous for the *CLCN7* variant, was most likely caused by bone marrow failure, a common phenotype of *CLCN7*-related osteopetrosis. Although bone marrow aplastic anaemia and myelodysplastic syndrome can also cause pancytopenia, the pathological results of bone marrow aspiration do not support this possibility. Additionally, III-3 had bilateral finger deformities, which were identified through family recall. Unfortunately, her systemic skeletal phenotype and imaging findings were not available because III-3 had passed away. According to her clinical *CLCN7*-related phenotype, onset in adulthood, and novel frameshift variant in *CLCN7* corresponding to the bone marrow failure phenotype [1, 10, 16], the ADO-II subtype of OP was the most

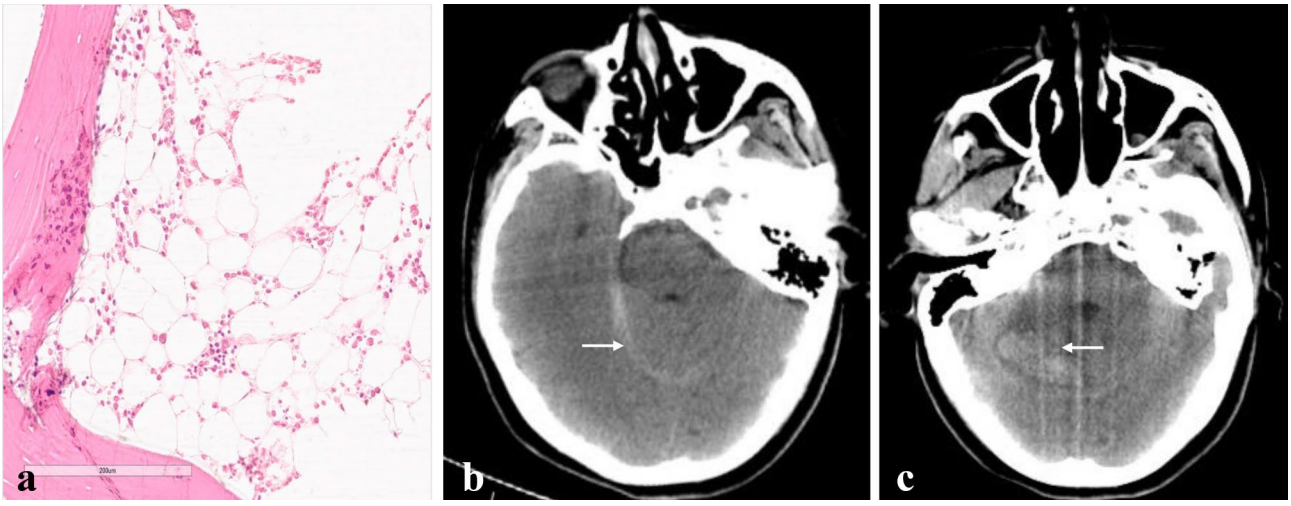


**Fig. 3** Examination results of the proband's mother (III-3). (**a**) Pathological results of bone marrow aspiration: bone marrow failure with decreased number of blood cells. (**b**) Focal hyperdense shadow in the right tentorium. (**c**) Right cerebellar hemorrhage (white arrows)

likely diagnosis of III-3, and the variant p.Met59Asnfs*8 was very likely responsible for its clinical phenotype. In addition, except for III-3, who presented a series of clinical phenotypes caused by bone marrow failure, all other family members (III-1, III-2, and IV-2) who were heterozygous had no obvious abnormal phenotypes, suggesting that the phenotype caused by the p.Met59Asnfs*8 variant of *CLCN7* exhibited incomplete dominance, which was consistent with the 44% penetrance of ADO-II related to *CLCN7* [16].

At both the international and domestic levels, the phenotypes of *CLCN7*-related ARO, IARO and ADO-II have been reported to be highly heterogeneous in previous studies [1, 20, 23]. However, there are no significant characteristic differences between countries and regions [1, 20, 23]. Compared with the limited clinical symptoms of the mother (III-3), who was heterozygous, the proband had a more comprehensive phenotype characteristic of ADO-II. Almost all typical skeletal phenotypes of ADO-II, such as bone pain, pathological fractures, degenerative joint disease, myelosuppression, and osteomyelitis, were observed in the proband, who was homozygous for the variant (Figs. 1 and 2) [1, 10, 15]. In addition, atypical phenotypes involving the haematopoietic, neurological, and dental systems, including anaemia, leukopenia, thrombocytopenia, hepatosplenomegaly, deafness, visual impairment, dental caries, missing teeth and malocclusion, were also observed in the proband (Figs. 1, 2 and 3; Table 1) [10, 11, 24–26]. Considering that the above-mentioned LOF via NMD was likely to be the underlying pathogenic mechanism of variant p.Met59Asnfs*8, we speculated that the differences in the range, age of onset, and severity of phenotypes between heterozygotes and homozygotes in this study were most likely related to the dose effect of LOF. The milder phenotype of mother (III-3) was very likely the result of haploinsufficiency caused by single-stranded heterozygous variant in *CLCN7*, as described previously [16, 19]. The more severe phenotype of the proband (IV-1) may be the result of a complete LOF caused by double-stranded homozygous variant (Fig. 4) [27].

Deafness can occur in ADO, ARO and IARO [26], and the type of deafness depends on the inheritance pattern and the responsible gene. Hearing loss caused by recessive inheritance typically involves mutations in *TCIRG1,CAII*, and *CLCN7* but is usually associated with other clinical symptoms [20]. Among the types of deafness caused by dominant inheritance, deafness in ADO-I due to mutations in *LRP5* is mostly conductive hearing loss, whereas deafness in ADO-II associated with mutations in *CLCN7* is mostly sensorineural hearing loss, which may be caused by skull sclerosis compressing the auditory nerve [28]. In our study, the proband presented with moderate to severe mixed deafness (Fig. 1b), which may also be associated with sclerosis of the ossicular chain (Fig. 2i and j) and dysfunction of V-ATPase in the epithelial cells of the inner ear endolymphatic sac [14, 16, 18, 29]. Cleft palate has not been reported to be associated with ADO-II but has been found in a patient with suspected ADO-I [30]. Whether cleft palate was a novel phenotype of *CLCN7*-related ADO-II needs to be confirmed by future studies.

To improve severe haemolytic anaemia, pancytopenia, splenomegaly caused by bone marrow cavity occlusion, impaired haematopoiesis, extramedullary haematopoiesis, and hypersplenism, the proband underwent splenectomy at the age of 3 years [31]. Encouragingly, the postoperative haematological parameters significantly improved (Table 1), and severe complications such as intracranial haemorrhage were avoided [32]. Although

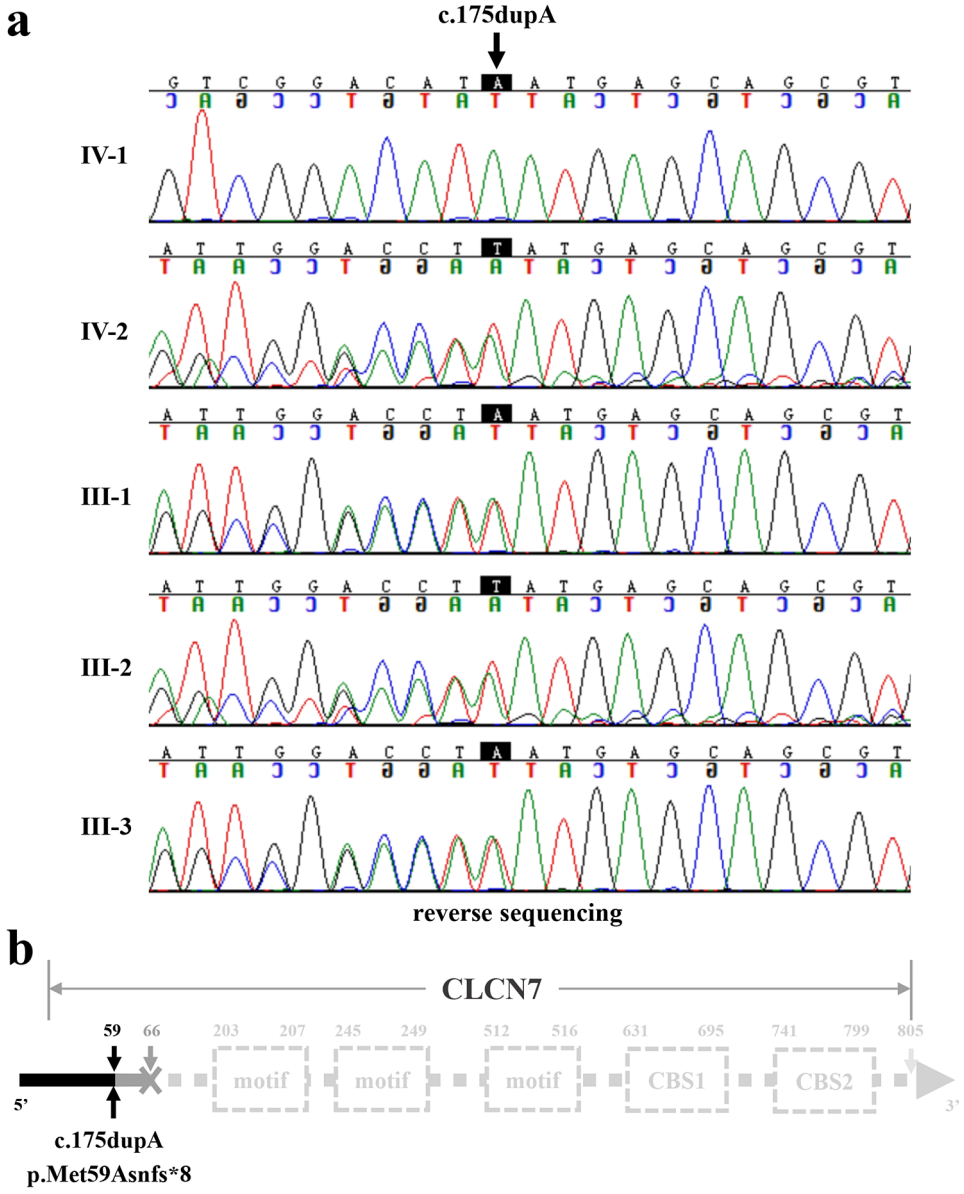


**Fig. 4** The p.Met59Asnfs*8 variant identified in Family. (**a**) Chromatograms showing the frameshift variant c.175dupA (p.Met59Asnfs*8). IV-1 with homozygote; III-1, III-2, III-3 and IV-2 with heterozygote. (**b**) Diagram of the mutant protein structure. The p.Met59Asnfs*8 variant led to the change of amino acid sequence from codon 59 and following by a stop at codon 66

the proband's mother experienced adult-onset disease, pancytopenia caused by bone marrow failure and secondary splenomegaly were not treated in time, and she eventually died of cerebellar haemorrhage [16]. We suggested that early splenectomy may prevent deaths with severe haemorrhagic causes, such as intracranial haemorrhage. In addition, after resection of the right infraorbital cyst, the proband experienced recurrent infection in the surgical area (Fig. 1c), which eventually spread to the intracranial region and resulted in death [33]. Owing to increased bone mineral density, narrow bone marrow cavities and poor blood supply [1], patients with OP are prone to secondary chronic osteomyelitis, resulting in infection after surgery [34]. Therefore, to avoid serious postoperative infections, operations adjacent to skeletal tissues in patients with OP should be avoided unless it would otherwise be fatal [33].

Although no phenotype was observed in the paternal aunt (III-1) or younger brother (IV-2), who were heterozygous, their offspring had a 50% chance of being carriers [1, 35]. Given the genetic background and incomplete penetrance of the phenotype, offspring carriers may still have a lethal OP phenotype [16]. Therefore, genetic counselling was needed for all offspring of the proband and carriers to avoid disease recurrence.

## Conclusion

In conclusion, the novel frameshift variant p.Met59Asnfs*8 in *CLCN7* identified in this study was very likely the disease-causing variant in our suspected ADO-II family. The phenotypes of heterozygous carriers may indicate incomplete penetrance. Loss of function of CLCN7 caused by NMD due to a frameshift variant was likely the underlying pathogenic mechanism. Timely splenectomy was a better intervention for prolonging the life of patients with severe anaemia, thrombocytopenia, and splenomegaly. Non-life-threatening surgeries adjacent to the skeletal tissue should be avoided as much as possible. This study broadened the mutation spectrum of *CLCN7*, presented a theoretical basis for genetic counselling and prenatal diagnosis, and provided guidance for clinical diagnosis and treatment.

**Acknowledgements**
The authors would like to thank all family members who voluntarily participated in this research for providing blood samples and accepting related clinical examinations.

**Author contributions**
Conceived and designed the experiments: XP; performed the experiments: ML, HZ, ZL, RP, YN; analyzed the data: XP, ML, LY; performed HRCT and analyzed imaging: JX; evaluated phenotypes of skeletal system: ZZ; contributed reagents / materials / analysis tools: XP, ZZ, JX; wrote and submitted the manuscript: ML, HZ, ZL; revised all drafts of the manuscript and approved the final manuscript as submitted: XP.

**Funding**
This research was supported by grants from National Science Foundation of China (81700920 to Xiuhong Pang), Medical Research Project of Jiangsu Provincial Health and Health Commission (M2022067 to Xiuhong Pang), Taizhou Municipal Science and Technology support (Social Development) Project (TS202214 to Xiuhong Pang), Basic research project from Taizhou School of Clinical Medicine of Nanjing Medical University (TZKY20230103 to Xiuhong Pang), Research Project of the Affiliated Taizhou People's Hospital of Nanjing Medical University (ZL202207 to Zhixiang Li).

**Data availability**
All data in this study can be obtained by contacting with Xiuhong Pang (email: pxhzxy@163.com).

## Declarations

**Ethics approval**
Documented permission about identifiable patient images from the patients or legal guardians was supplied as patient consent form. This study was approved by the Ethics Committee of the Affiliated Taizhou People's Hospital of Nanjing Medical University (KY202012301; 22th October, 2020) and was compliance with the Declaration of Helsinki.

**Consent to participate**
All subjects or legal guardians in this study gave written, informed consent to participate in this study. Identifying information will not be included in the manuscript unless the information is essential for scientific purposes.

**Competing interests**
The authors declare no competing interests.

**Author details**
[1]Department of Otorhinolaryngology-Head and Neck Surgery, The Affiliated Taizhou People's Hospital of Nanjing Medical University, Taizhou School of Clinical Medicine, Nanjing Medical University, Taizhou, Jiangsu, China
[2]Department of Otorhinolaryngology-Head and Neck Surgery, the Affiliated Taizhou People's Hospital of Nanjing Medical University, Taizhou, Jiangsu, China
[3]Department of Otorhinolaryngology-Head and Neck Surgery, Postgraduate Training Base of Dalian Medical University (Taizhou People's Hospital), Taizhou, Jiangsu, China
[4]Department of Otolaryngology Head and Neck Surgery, Nanjing Drum Tower Hospital, Clinical Medical College of Traditional Chinese and Western Medicine, Nanjing University of Chinese Medicine, Nanjing, Jiangsu, China
[5]Department of Osteology, The Affiliated Taizhou People's Hospital of Nanjing Medical University, Taizhou, Jiangsu, China
[6]Department of Imaging, The Affiliated Taizhou People's Hospital of Nanjing Medical University, Taizhou, Jiangsu, China

Received: 11 March 2024 / Accepted: 5 February 2025
Published online: 24 February 2025

**References**

1. Polgreen LE, Imel EA, Econs MJ. Autosomal dominant osteopetrosis. Bone. 2023;170:116723.
2. Del Fattore A, Cappariello A, Teti A. Genetics, pathogenesis and complications of osteopetrosis. Bone. 2008;42(1):19–29.
3. Palagano E, Menale C, Sobacchi C, Villa A. Genetics of Osteopetrosis. Curr Osteoporos Rep. 2018;16(1):13–25.
4. Tuysuz B, Usluer E, Uludag Alkaya D, Ocak S, Saygili S, Seker A, Apak H. The molecular spectrum of Turkish osteopetrosis and related osteoclast disorders with natural history, including a candidate gene, CCDC120. Bone. 2023;177:116897.
5. Nadyrshina DD, Khusainova RI. Clinical, genetic aspects and molecular pathogenesis of osteopetrosis. Vavilovskii Zhurnal Genet Selektsii. 2023;27(4):383–92.
6. Wei A, Zhu GH, Qin MQ, Jia CG, Wang B, Yang J, Luo YH, Jing YF, Yan Y, Zhou X, et al. [Analysis of clinical presentation and genetic characteristics of malignant infantile osteopetrosis]. Zhonghua Er Ke Za Zhi. 2023;61(11):1038–42.
7. Jodeh W, Katz AJ, Hart M, Warden SJ, Niziolek P, Alam I, Ing S, Polgreen LE, Imel EA, Econs MJ. Autosomal Dominant Osteopetrosis (ADO) caused by a missense variant in the TCIRG1 gene. J Clin Endocrinol Metab. 2024;109(7):1726–32.
8. Kheir V, Munier FL, Aubry-Rozier B, Schorderet DF. Potential blindness in children of patients with hereditary bone disease. Osteoporos Int. 2016;27(2):841–4.
9. Gong HP, Ren Y, Zha PP, Zhang WY, Zhang J, Zhang ZW, Wang C. Clinical and genetic diagnosis of autosomal dominant osteopetrosis type II in a Chinese family: a case report. World J Clin Cases. 2023;11(3):700–8.
10. Bailey JR, Tapscott DC. Osteopetrosis. *StatPearls*. Treasure Island (FL) ineligible companies. Disclosure: David Tapscott declares no relevant financial relationships with ineligible companies.; 2024.
11. Stauber T, Wartosch L, Vishnolia S, Schulz A, Kornak U. CLCN7, a gene shared by autosomal recessive and autosomal dominant osteopetrosis. Bone. 2023;168:116639.
12. Calder AD, Arulkumaran S, D'Arco F. Imaging in osteopetrosis. Bone. 2022;165:116560.
13. Song XL, Peng LY, Wang DW, Wang H. Autosomal dominant osteopetrosis type II resulting from a de novo mutation in the CLCN7 gene: a case report. World J Clin Cases. 2022;10(20):6936–43.
14. Bose S, de Heus C, Kennedy ME, Wang F, Jentsch TJ, Klumperman J, Stauber T. Impaired Autophagic Clearance with a Gain-of-Function Variant of the Lysosomal Cl(-)/H(+) Exchanger ClC-7. Biomolecules 2023, 13(12).
15. Rossler U, Hennig AF, Stelzer N, Bose S, Kopp J, Soe K, Cyganek L, Zifarelli G, Ali S, von der Hagen M, et al. Efficient generation of osteoclasts from human induced pluripotent stem cells and functional investigations of lethal CLCN7-related osteopetrosis. J Bone Min Res. 2021;36(8):1621–35.
16. Zifarelli G. The role of the lysosomal Cl(-)/H(+) antiporter ClC-7 in Osteopetrosis and neurodegeneration. Cells 2022, 11(3).
17. Bose S, He H, Stauber T. Neurodegeneration upon Dysfunction of Endosomal/Lysosomal CLC Chloride transporters. Front Cell Dev Biol. 2021;9:639231.
18. Chen F, Kang R, Liu J, Tang D. The V-ATPases in cancer and cell death. Cancer Gene Ther. 2022;29(11):1529–41.

19. Cao X, Lenk GM, Mikusevic V, Mindell JA, Meisler MH. The chloride antiporter CLCN7 is a modifier of lysosome dysfunction in Fig. 4 and VAC14 mutants. PLoS Genet. 2023;19(6):e1010800.
20. Sobacchi C, Villa A, Schulz A, Kornak U. CLCN7-Related Osteopetrosis. In: *GeneReviews((R))*. Edited by Adam MP, Feldman J, Mirzaa GM, Pagon RA, Wallace SE, Amemiya A. Seattle (WA); 1993.
21. Nagy E, Maquat LE. A rule for termination-codon position within intron-containing genes: when nonsense affects RNA abundance. Trends Biochem Sci. 1998;23(6):198–9.
22. Kornak U, Kasper D, Bosl MR, Kaiser E, Schweizer M, Schulz A, Friedrich W, Delling G, Jentsch TJ. Loss of the ClC-7 chloride channel leads to osteopetrosis in mice and man. Cell. 2001;104(2):205–15.
23. Funck-Brentano T, Zillikens MC, Clunie G, Siggelkow H, Appelman-Dijkstra NM, Cohen-Solal M. Osteopetrosis and related osteoclast disorders in adults: a review and knowledge gaps on behalf of the European calcified tissue society and ERN BOND. Eur J Med Genet. 2024;69:104936.
24. Di Zanni E, Palagano E, Lagostena L, Strina D, Rehman A, Abinun M, De Somer L, Martire B, Brown J, Kariminejad A, et al. Pathobiologic Mechanisms of Neurodegeneration in Osteopetrosis Derived from Structural and Functional Analysis of 14 ClC-7 mutants. J Bone Min Res. 2021;36(3):531–45.
25. Guo X, Duan X. Genotype-phenotype analysis of selective failure of tooth eruption-A systematic review. Clin Genet. 2023;104(3):287–97.
26. Ma Y, Xu Y, Zhang Y, Duan X. Molecular mechanisms of Craniofacial and Dental abnormalities in Osteopetrosis. Int J Mol Sci 2023; 24(12).
27. Hofstaetter JG, Atkins GJ, Kato H, Kogawa M, Blouin S, Misof BM, Roschger P, Evdokiou A, Yang D, Solomon LB, et al. A mild case of autosomal recessive osteopetrosis masquerading as the Dominant Form Involving homozygous deep intronic variations in the CLCN7 gene. Calcif Tissue Int. 2022;111(4):430–44.
28. Steward CG. Neurological aspects of osteopetrosis. Neuropathol Appl Neurobiol. 2003;29(2):87–97.
29. Teti A, Whyte MP. Osteopetrosis: gene-based nosology and significance. Bone. 2023;175:116854.
30. Kim JK, Kim JY, Jung HD, Jung YS. Surgical-orthodontic treatment for severe malocclusion in a patient with osteopetrosis and bilateral cleft lip and palate. Angle Orthod. 2021;91(4):555–63.
31. Whyte MP. Osteopetrosis: Discovery and early history of marble bone disease. Bone. 2023;171:116737.
32. Adams BK, Smuts NA. The detection of extramedullary hematopoiesis in a patient with osteopetrosis. Eur J Nucl Med. 1989;15(12):803–4.
33. Sabacinski K, Booth M, Bramer M. Managing osteopetrosis in the Complex Polytrauma Orthopedic Patient. Cureus. 2022;14(2):e21886.
34. Lamut A, Kovac S. Complications of surgical management of osteopetrosis. A case report of multiple surgeries performed on one patient. J Surg Case Rep. 2023;2023(5):rjad315.
35. Wang Z, Li X, Wang Y, Fu W, Liu Y, Zhang Z, Wang C. Natural history of type II autosomal Dominant osteopetrosis: a single Center Retrospective Study. Front Endocrinol (Lausanne). 2022;13:819641.

## Publisher's note